Genetic factors influencing a neurobiological substrate for psychiatric disorders

Till F. M. Andlauer[1,2,*], Thomas W. Mühleisen[3,4,5,*], Felix Hoffstaedter[3], Alexander Teumer[6], Katharina Wittfeld[7,8], Anja Teuber[9,10], Céline S. Reinbold[5,11], Robin Bülow[12], Svenja Caspers[3,13], Stefan Herms[5,14], Per Hoffmann[3,5,14,15], Heike Minnerup[9], Susanne Moebus[16], Henning Teismann[9], Uwe Völker[17], International FTD-Genomics Consortium (IFGC), The 23andMe Research Team, Amit Etkin[18-20], Klaus Berger[9], Hans J. Grabe[21], Markus M. Nöthen[14,15], Katrin Amunts[3,4,22], Simon B. Eickhoff[3,23], Philipp G. Sämann[1], Bertram Müller-Myhsok[1,24,*], Sven Cichon[3,5,25,*]

[1]Max Planck Institute of Psychiatry, Munich, Germany;
[2]Department of Neurology, Klinikum rechts der Isar, School of Medicine, Technical University of Munich, Munich, Germany;
[3]Institute of Neuroscience and Medicine (INM-1, INM-7), Research Centre Jülich, Germany;
[4]Cécile and Oskar Vogt Institute of Brain Research, Medical Faculty, Heinrich Heine University Düsseldorf, Düsseldorf, Germany;
[5]Department of Biomedicine, University of Basel, Switzerland;
[6]Institute for Community Medicine, University Medicine Greifswald, Germany;
[7]German Center for Neurodegenerative Diseases (DZNE), Site Rostock/Greifswald, Germany;
[8]Department of Psychiatry and Psychotherapy, University Medicine Greifswald, Greifswald, Germany;
[9]Institute of Epidemiology and Social Medicine, University of Münster, Münster, Germany;
[10]Institut für Energie- und Umwelttechnik e.V. (IUTA, Institute of Energy and Environmental Technology), Duisburg, Germany;
[11]Center for Lifespan Changes in Brain and Cognition, Department of Psychology, University of Oslo, Oslo, Norway;
[12]Institute of Diagnostic Radiology and Neuroradiology, University Medicine Greifswald, Germany;
[13]Institute for Anatomy I, Medical Faculty, Heinrich Heine University Düsseldorf, Düsseldorf, Germany;
[14]Department of Genomics, Life & Brain Center, University of Bonn, Germany;
[15]Institute of Human Genetics, University of Bonn, Germany;
[16]IMIBE, University Hospital of Essen, University Duisburg-Essen, Germany;
[17]Interfaculty Institute for Genetics and Functional Genomics, University Medicine Greifswald, Germany;
[18]Department of Psychiatry and Behavioral Sciences, Stanford University, Stanford, CA, 94304, USA;
[19]Wu Tsai Neurosciences Institute, Stanford University, Stanford, CA, 94304, USA
[20]Veterans Affairs Palo Alto Healthcare System, and the Sierra Pacific Mental Illness, Research, Education, and Clinical Center (MIRECC), Palo Alto, CA, 94394, USA;
[21]Department of Psychiatry and Psychotherapy, University Medicine Greifswald, Greifswald, Germany;
[22]JARA-Brain, Jülich-Aachen Research Alliance, Jülich, Germany;
[23]Institute of Clinical Neuroscience and Medical Psychology, Heinrich-Heine University, Düsseldorf, Germany;
[24]Institute of Translational Medicine, University of Liverpool, United Kingdom;
[25]Institute of Medical Genetics and Pathology, University Hospital Basel, Switzerland.

*These authors have contributed equally.

1

Correspondence should be addressed to:
Sven Cichon
Institute of Neuroscience and Medicine (INM-1)
Research Centre Jülich
Leo-Brandt-Strasse
D-52428 Jülich
Germany
E-mail: s.cichon@fz-juelich.de
Telephone: +41 61 265 36 47

Running title:
Genetics of a psychiatric cross-disorder MRI substrate

Abstract

Background:
Evidence from meta-analyses of MRI-based brain morphometry suggested a common neurobiological substrate (CS) for psychiatric disorders in the dorsal anterior cingulate (dACC) and the anterior insular cortices (AIC).

Methods:
We analyzed the first principal component of voxel-based morphometric volumes forming the CS (hereafter abbreviated as CCS). We conducted genome-wide association studies (GWAS) of the CCS in four cohorts (discovery, n=2,271), followed by meta-analysis, and replication in a fifth cohort (n=865). Secondary genetic and clinical imaging analyses were performed in two major depressive disorder case/control cohorts (n=967 cases and n=508 controls).

Results:
The single-nucleotide polymorphism (SNP) rs17076061 on chromosome 5q35.2 was associated with the CCS at genome-wide significance and replicated. Psychiatric cross-disorder polygenic risk scores were associated with the CCS at nominal significance. However, no significant genome-wide overlap between genetic variants influencing the CCS and genetic risk for different disorders was found after correction for multiple testing. Further secondary analyses revealed a dependence of the association of the identified variant on interactions with age.

Conclusions:
We identified a significant association between a genetic variant and a transdiagnostic psychiatric marker. The SNP maps to a locus harboring genes involved in neuronal development and regeneration. Dependence of this association on age and the absence of direct associations with major psychiatric disorders suggest an indirect relationship between the CCS and disease risk, contingent on environmental and additional, unknown genetic factors. Overall, our study indicates a complex interplay between common genetic variation and the function of brain regions affected in psychiatric patients.

Introduction

Numerous studies have identified regional differences in the brain structure of psychiatric patients and described both transdiagnostic and disorder-specific processes of gray matter (GM) reduction in patients (1–9). However, the biological mechanisms contributing to such clinically relevant regional GM differences are mostly unclear. One possibility is that GM loss occurs as a consequence of disease manifestation. Alternatively, as a genetic influence on cortical and subcortical brain regions is well documented (10–16), GM changes may precede the onset of psychopathology and directly increase disease risk. A third explanation is that reduced GM volume in patients constitutes a regional vulnerability. In this model, the susceptibility to develop psychiatric symptoms would increase if genetic risk factors and unfavorable environmental factors or aging processes jointly affect specific brain regions.

In a large meta-analysis of 193 imaging studies, Goodkind and colleagues found that GM volumes obtained from structural magnetic resonance imaging (MRI) using voxel-based morphometry (VBM) were reduced across six psychiatric diagnoses in parts of the bilateral anterior insular cortex (AIC) and the dorsal anterior cingulate cortex (dACC)(1). Structural and functional connectivity analyses supported that these regions are tightly connected and represent hubs of the salience network (1). Functional differences in salience processing in these brain regions are associated with diagnostic status and progression of psychiatric disorders (17). The authors hypothesized that the regions jointly form a common neurobiological substrate (CS) of major psychiatric disorders (1).

Many studies analyzed genetic risk factors for major psychiatric disorders like schizophrenia, bipolar disorder (BD), and major depressive disorder (MDD). These disorders show substantial heritability (18) and are genetically correlated with each other (19). Genome-wide association studies (GWAS) identified single-nucleotide polymorphisms (SNPs) contributing risk for several psychiatric disorders, suggesting pleiotropy and partially overlapping etiologies (20, 21). While some studies reported partial overlaps between brain volume-associated and disease-associated SNPs, others did not (2, 10, 22–24).

The present study aimed to identify genetic variants influencing the CS in the general population. To this end, a combined VBM measure of the three CS regions (hereafter referred to as the first principal component of the CS, *CCS*), was computed in five population-based cohorts. Meta-analyses of GWAS conducted in these cohorts identified a novel locus significantly associated with the CCS. In secondary analyses, genetic relationships between the CCS and risk for psychiatric disorders were characterized in detail, emphasizing a potentially modulating role of age on the CCS.

3

Methods and Materials

Sample description

For the GWAS, n=3,136 individuals from five population-based cohorts were investigated. Four cohorts were used in the discovery (1000BRAINS(25), n=539; CONNECT100 (26), n=93; BiDirect (27), n=589; SHIP-2 (28), n=1,050; pooled n=2,271) and the second-largest cohort available in the replication stage (SHIP-Trend (28), n=865). For follow-up analyses, two MDD cohorts with 967 cases and 508 controls were used, BiDirect (29) (n=582 MDD cases; n=311 controls) and MPIP (30, 31) (n=385 MDD cases; n=197 controls). Basic demographic characteristics of the cohorts are described in Tables S1 and S2. The studies were approved by the local ethics committees; all participants provided written informed consent.

VBM preprocessing and extraction of regional and total GM volumes

VBM preprocessing (32, 33) was applied to high-resolution T1-weighted images from all participants to create GM maps with non-linear only (NLO) Jacobian modulation. Three spatially disjunct regional GM volumes, based on binarized versions of the joint result areas from the study by Goodkind *et al.* (1), and total GM volume were extracted.

All GM volumes were corrected for age, age×age, and sex in multiple linear regression models. Handedness was used as an additional covariate for 1000BRAINS, CONNECT100, and BiDirect, and coil type for the MPIP sample. Residuals of these regional volume regression models were combined using principal component analysis (PCA) to create a single measure referred to as the *Component of the Common Substrate* (CCS; Fig. 1).

Genotyping, quality control, and imputation

DNA extraction and genome-wide genotyping were conducted as described before (31, 34–36). Genotyping was carried out on different Illumina and Affymetrix microarrays (see the Supplemental Methods and Table S3). Quality control (QC) and imputation were conducted separately for each genotyping batch, using the same protocols, in PLINK (37), *R*, and XWAS (38); genotype data were imputed to the 1000 Genomes phase 1 reference panel using SHAPEIT and IMPUTE2 (39–41), as described in the Supplement and previously (42). The population substructure of all five cohorts is shown in Fig. S1.

Heritability estimation and GWAS

The SNP-based heritability of the CCS was estimated using GCTA on a combined sample of the imputed data from all five cohorts (43, 44) (see the Supplemental Methods). GWAS was conducted separately per cohort using PLINK with ancestry components as covariates. Variants on the X chromosome were analyzed separately by sex, followed by *p* value-based meta-analysis to allow for different effect sizes per sex. A two-stage design was implemented for the GWAS, using four cohorts as the discovery sample and SHIP-Trend as an independent replication sample. Cohorts were combined by fixed-effects meta-analysis using METAL (45). There was no indication for genomic inflation of the GWAS test statistics in the single cohorts or the meta-analysis (λ_{1000}=1.01, see Table S4 and Fig. S2).

Linkage disequilibrium (LD) was analyzed using the 1000 Genomes CEU population in LDmatrix (46). We carried the two SNPs forward to the replication stage that showed the most robust genome-wide support ($p<5\times10^{-8}$) for an association in

4

the discovery stage and were partially independent of each other (LD r^2<0.5 with more strongly associated variants). Here, a one-sided *p*-value <α=0.05/2 (correcting for two LD-independent variants) was considered as successful replication. See the Supplement for additional details.

Gene-set analyses

Gene-set analyses were conducted on the meta-analysis of the discovery- and replication-stage GWAS, using 674 REACTOME gene sets containing 10–200 genes curated from MsigDB 6.2 (47). Only SNPs within gene boundaries were mapped to RefSeq genes (0 bp window). Analyses were conducted in MAGMA v1.07 using both mean- and top-SNP gene models (48) and in MAGENTA v2 using a top-SNP approach (49). Here, false discovery rates were calculated to correct for multiple testing.

Comparison to published GWAS of psychiatric disorders

For genome-wide comparisons between our GWAS meta-analysis and published GWAS of psychiatric disorders, summary statistics from the following PGC GWAS were used: cross-disorder 2013 (50), BD 2019 (51), MDD 2018 (with 23andMe)

(52), and schizophrenia 2014 (53). For additional comparisons, the following GWAS were used: IFGC behavioral frontotemporal dementia (bvFTD) 2014 (54), longevity 85/90 2014 (55), and three different GWAS from 2017 on epigenetic accelerated aging (EAA) (56): EAA in all examined brain regions, EAA in prefrontal cortex (PC), and neuronal proportion in PC.

Polygenic risk scores (PRS) were calculated and analyzed in *R* using imputed genetic data (57). We ran LD score regression (LDSC) comparing the genetic correlation of published GWAS to the CCS GWAS summary statistics with standard settings (58, 59). We analyzed whether the order of SNPs ranked by their association strength was random between studies using rank-rank hypergeometric overlap (RRHO) tests (60). For this analysis, variants were LD-pruned in the 1000 Genomes phase 3 EUR subset (61). Binomial sign tests were conducted in *R* (*binom.test*) to analyze whether SNPs associated with the CCS at either *p*<0.05 or *p*<1×10^{-5} showed the opposite direction of effects in other GWAS more often than expected by chance. For additional details, see the Supplemental Methods.
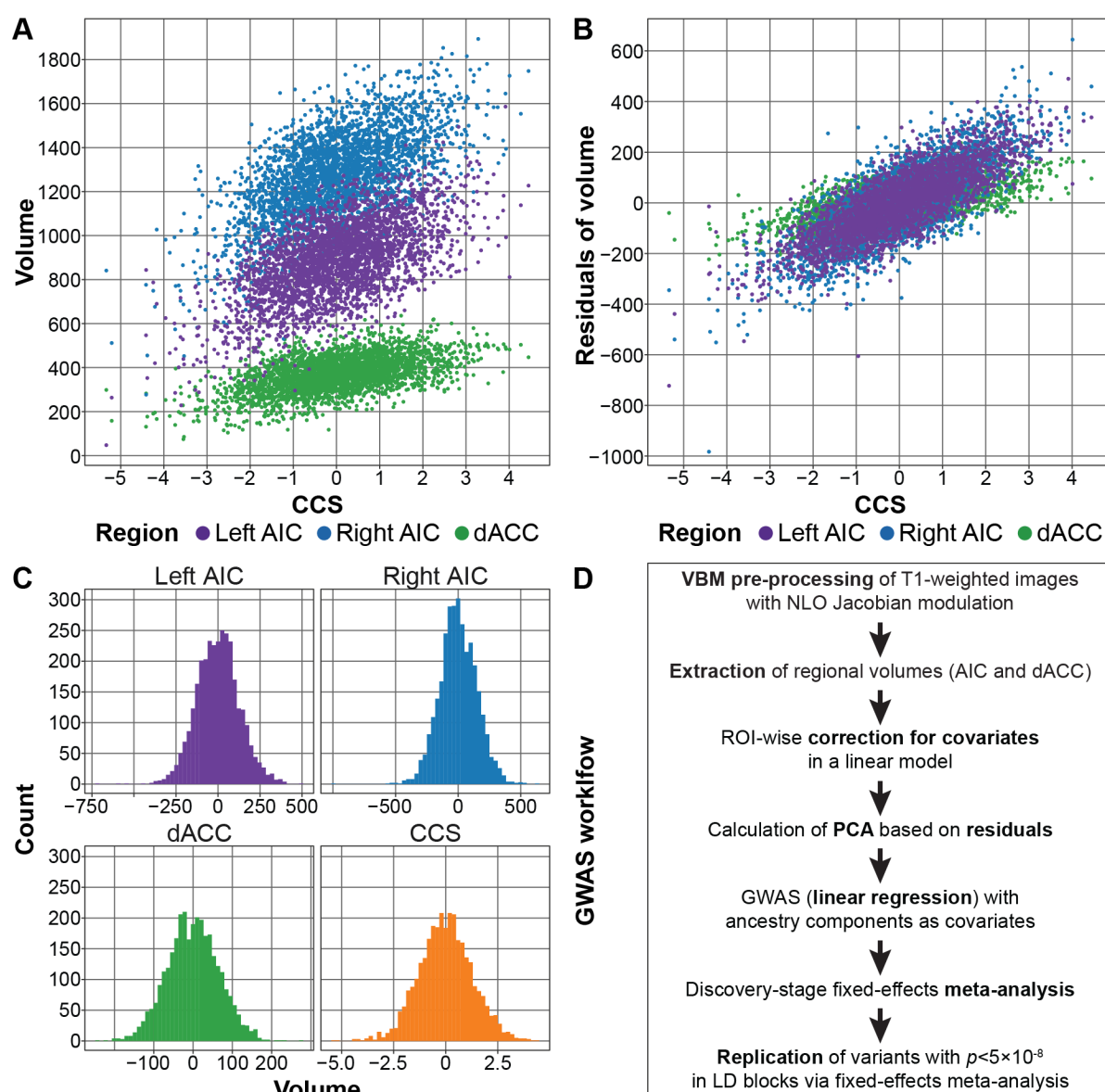
Figure 1: Generation of the CCS and GWAS analysis workflow.
A-B: Comparison between the CCS and the three individual volumes (A) and the residuals of the three volumes after correction for covariates (B). AIC = anterior insula cortex; dACC = dorsal anterior cingulate cortex **C:** Histograms of the three extracted volumes and the CCS. Note that A-C show combined data from all five GWAS cohorts. Correlations were left and right AIC: $r=0.65$, left AIC and dACC: $r=0.52$, right AIC and dACC: $r=0.46$. **D:** GWAS analysis workflow. All measures were extracted using NLO-based Jacobian modulation. All GM volumes were corrected for age, age^2, and sex as covariates; handedness was used as an additional covariate for the three samples 1000BRAINS, CONNECT100, and BiDirect. **PCA** = principal component analysis; **LD** = linkage disequilibrium.

Results

Heritability of the imaging CCS

After correction for covariates, the CCS showed a SNP heritability estimate of h^2_g=0.50 (standard error, SE=0.18; *p*-value=0.0033).

GWAS of the CCS

In the discovery-stage GWAS, twelve SNPs on chromosome *5q35.2* showed genome-wide significant associations with the CCS (*p*<5×10⁻⁸; Fig. 2A and Table S5). Most of these SNPs were highly correlated with each other (Table S6). The two partially LD-independent SNPs (pairwise LD *r²*=0.267 in CEU samples) with the most robust support for an association were analyzed further. Of these, variant rs17076061 was significantly associated in the replication cohort (discovery: *p*=1.51×10⁻⁸; replication: one-sided *p*=9.91×10⁻³) and also the top-associated variant in the genome-wide meta-analysis of discovery and replication samples (*p*=1.46×10⁻⁹; Table 1, Fig. 2B-D; Table S5 and Fig. S2-S4). This SNP was associated at genome-wide significance only for the CCS but not when examining either whole-brain GM volume or the three GM regions forming the CS separately (Table 1). The minor allele T of SNP rs17076061 (frequency = 0.36) is thus associated with smaller CS volumes.
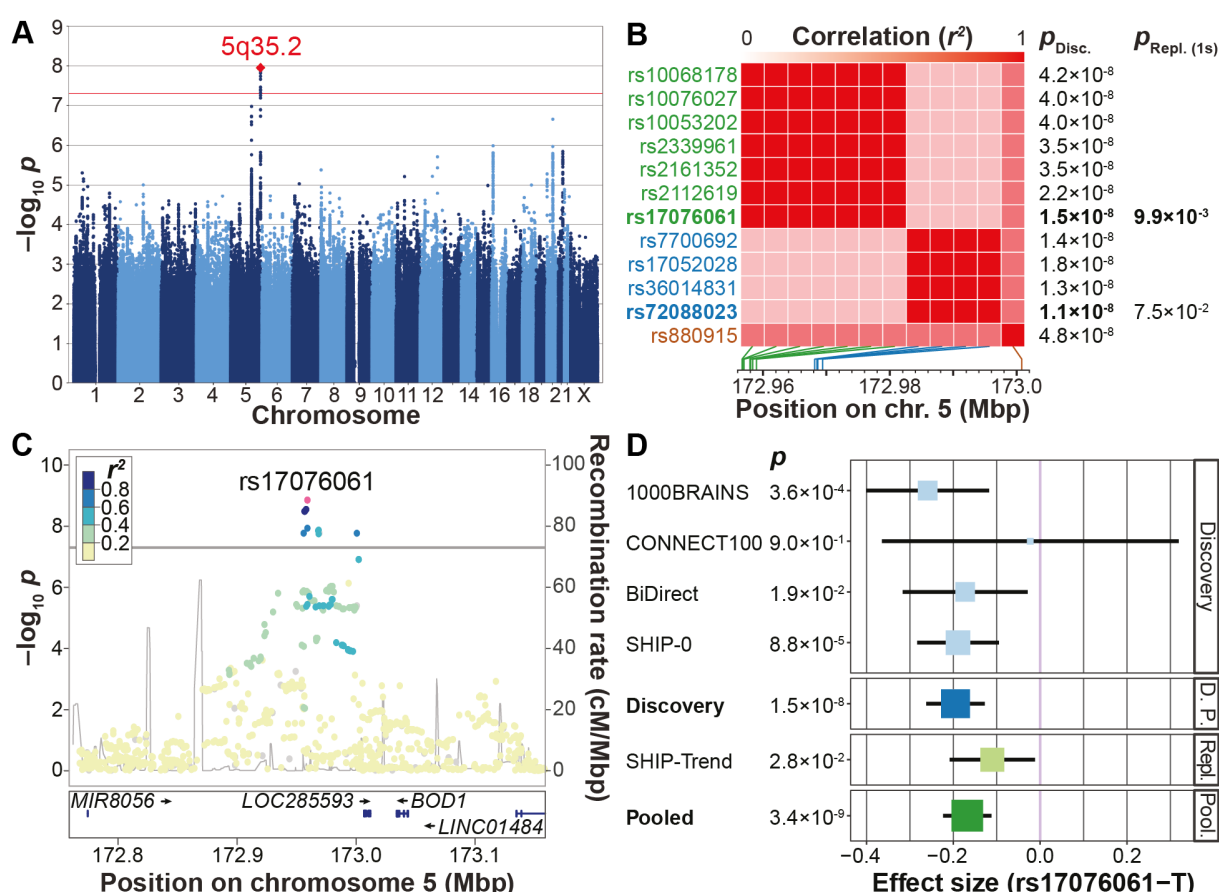

Figure 2: Presentation of GWAS results.
A: Manhattan plot showing the strength of evidence for an association (*p*-value) in the discovery stage CCS GWAS. Each variant is shown as a dot, with alternating shades of blue according to chromosome; the top-associated locus *5q32.2* is labeled with a red diamond. The red line marks the genome-wide significance level. **B:** Matrix of the pairwise LD pattern (1000 Genomes population CEU) between the twelve variants that

reached genome-wide significance in the discovery GWAS. The two variants rs17076061 and rs72088023 (r^2=0.267) showed the strongest support for an association in their respective LD blocks and were analyzed in the replication stage. All other variants had pairwise LD>0.5 with either of these two variants, their association strengths are provided for comparison only. $p_{Disc.}$: discovery stage GWAS *p*-value; $p_{Repl. (1s)}$: one-sided *p*-value in the replication cohort; Mbp: mega base pair. **C:** Regional association plot of the top-associated locus after pooled analysis of the discovery stage GWAS and the replication sample. The color of dots indicates LD with the lead variant (rs17076061; pink). Gray dots represent signals with missing LD r^2 values. cM: centimorgan. **D:** Forest plot of the pooled analysis of the replicated variant rs17076061 in discovery and replication cohorts. D. P.: pooled analysis of discovery stage cohorts; Repl.: replication; Pool.: pooled analysis of the discovery GWAS and the replication cohort SHIP-Trend.

rs17076061	Effect size	SE	*p*-value
CCS	-0.21	0.03	$1.46×10^{-9}$
Left AIC	-17.96	3.36	$8.79×10^{-8}$
Right AIC	-17.78	3.87	$4.34×10^{-6}$
dACC	-5.48	1.74	$1.64×10^{-3}$
Total gray matter	-4.17	1.09	$1.36×10^{-4}$

Table 1: Association results from the genome-wide meta-analysis of discovery and replication samples.
The effect size refers to the minor allele T. All measures were extracted using non-linear only (NLO)-based Jacobian modulation. **AIC** = anterior insula cortex; **dACC** = dorsal anterior cingulate cortex; **SE** = standard error.

Gene-set analyses
In two separate gene-set analyses using GWAS meta-analysis results, the top-associated pathway, significant after correction for multiple testing, was "SEMA3A-Plexin repulsion signaling by inhibiting Integrin adhesion" (Tables S7-S8, https://www.reactome.org/content/detail/R-HSA-399955).

Comparisons of the CCS and the CCS genetic architecture with psychiatric disorders
To characterize the relationship between the CCS and risk for psychiatric disorders, we tested whether results from our CCS GWAS overlapped with results from four published GWAS of psychiatric disorders (PGC cross-disorder (50), BD (51), MDD (52), and schizophrenia (53)). SNP rs17076061 was not significantly associated with disorders in any of these GWAS (*p*>0.26, Table S9).

We ran four separate systematic comparisons with the psychiatric GWAS, following a published workflow (22): First, we calculated PRS using the four GWAS as training data and analyzed associations of these PRS with the CCS. Although the cross-disorder PRS showed a nominally significant association with a smaller CCS at a single PRS threshold (one-sided *p*=0.01), none of the PRS were significantly associated after correction for multiple testing (Table 2; Table S10 and Fig. S5). We also calculated a CCS PRS in an independent MDD case/control sample (MPIP). However, the CSS PRS was not significantly higher in MDD cases at any threshold (one-sided *p*≥0.55, Table S11). Second, no significant genetic correlation was found between the CCS GWAS and

any of the psychiatric GWAS using LDSC (Table 2, Table S12). Third, no significant overlap of SNPs ranked by association strength was found with RRHO tests (Table 2; Table S13, and Fig. S6). Fourth, we carried out binomial sign tests and found that CCS-associated variants did not show the opposite effect direction in the psychiatric disorder GWAS more often than expected by chance (Table 2 and Table S14).

Polygenic risk scores (PRS)

Training GWAS	Effect size	*p*-value	p_T
Psychiatric Cross-Disorder	-2.24	0.01	1×10^{-4}
Bipolar Disorder	-0.64	0.05	1×10^{-7}
Major Depression	-5.01	0.31	1×10^{-2}
Schizophrenia	-0.58	0.24	1×10^{-7}

LD score regression (LDSC)

GWAS comparison	r_g	*p*-value
Psychiatric Cross-Disorder	0.18	0.15
Bipolar Disorder	0.17	0.08
Major Depression	-0.03	0.75
Schizophrenia	0.08	0.38

Rank-rank hypergeometric overlap (RRHO)

GWAS comparison	Overlap	*p*-value
Psychiatric Cross-Disorder	0.06	0.57
Bipolar Disorder	0.21	0.06
Major Depression	0.04	0.18
Schizophrenia	0.02	0.15

Binomial sign tests (*p*<0.05)

GWAS comparison	Probability	*p*-value
Psychiatric Cross-Disorder	0.50	0.68
Bipolar Disorder	0.50	0.67
Major Depression	0.50	0.82
Schizophrenia	0.50	0.64

Binomial sign tests (*p*<1×10^{-5})

GWAS comparison	Probability	*p*-value
Psychiatric Cross-Disorder	0.50	0.75
Bipolar Disorder	0.54	0.50
Major Depression	0.33	0.93
Schizophrenia	0.54	0.50

Table 2: Comparisons of the CCS and the CCS genetic architecture with psychiatric disorders.
For detailed results see Tables S10-S13. Details on the four training GWAS datasets are provided in the Methods section. **PRS:** Association of polygenic risk scores with the CCS; *pT* = training GWAS data *p*-value threshold; effect size = linear regression effect size at the *pT* showing the strongest support for an association (see Table S10

for results of all ten thresholds); *p*-value: one-sided *p*-value not corrected for multiple testing. The significance level adjusted for multiple testing was α=0.05/(10×4) =0.00125. **LDSC:** LD score regression using genome-wide summary statistics; r_g = genetic correlation. **RRHO:** Rank-rank hypergeometric overlap test showing the relative overlap of genome-wide summary statistics. **Sign tests:** One-sided binomial sign tests for CCS GWAS *p*-value thresholds $p<0.05$ and $p<1\times10^{-5}$ and the corresponding probability of success.

Analyses of age-dependent effects

We confirmed in two MDD case/control cohorts that the CSS was reduced in cases ($p=3\times10^{-6}$, Fig. 3A, Table S15). We did not observe a significant age-by-diagnosis interaction in this analysis ($p=0.07$). However, when including such an interaction term, the main effect of MDD diagnosis did not remain significant either ($p=0.10$, Fig. 3B; Fig. S7, and Table S15). To test for a non-linear age dependency, we stratified the cohorts into four age groups (see Fig. 3C). Effect sizes differed between age groups but without showing significant heterogeneity in a meta-analysis across the groups ($Q=3.55$, $p=0.31$; Fig. 3C, Table S16). The association of the CCS with MDD may thus, potentially, be age-dependent.

When adding an age-by-SNP interaction term to the GWAS model, this term was not significant in the meta-analysis of all five cohorts ($p=0.96$, Fig. S8, and Table S17) but the main effect of variant rs17076061 also did not remain significant (p=0.27, compared to $p=1.46\times10^{-9}$ without the interaction in the model). When we stratified the analysis by age groups, the effect size varied, yet without significant heterogeneity ($Q=2.25$, $p=0.69$; Fig. 3D, Table S16).

We investigated whether the global brain volume correction intrinsically contained in NLO Jacobian modulation may have caused these effects. However, results were highly similar when using full Jacobian modulation with total intracranial volume added as a covariate to the regression model for explicit correction of global volume (Supplemental Methods and Table S17).

Comparison of the genetic architecture of the CCS and aging-related traits

Due to a potential effect of aging on the CCS, we compared our CCS GWAS with GWAS for EAA (56) and longevity (55). Furthermore, since the CS regions are central to the salience network, we also analyzed the overlap with GWAS results for bvFTD (54). SNP rs17076061 did not show a significant association in any of these GWAS (Table S9). No significant genetic overlap with any of these GWAS was found after correction for multiple testing, using PRS analyses, LDSC, RRHO, or sign tests (Figs. S5 and S9 and Tables S10 and S12-S14). However, here we observed several nominally significant associations and genetic overlaps, indicating that a weak genetic relationship between the CCS and aging-associated traits might exist.
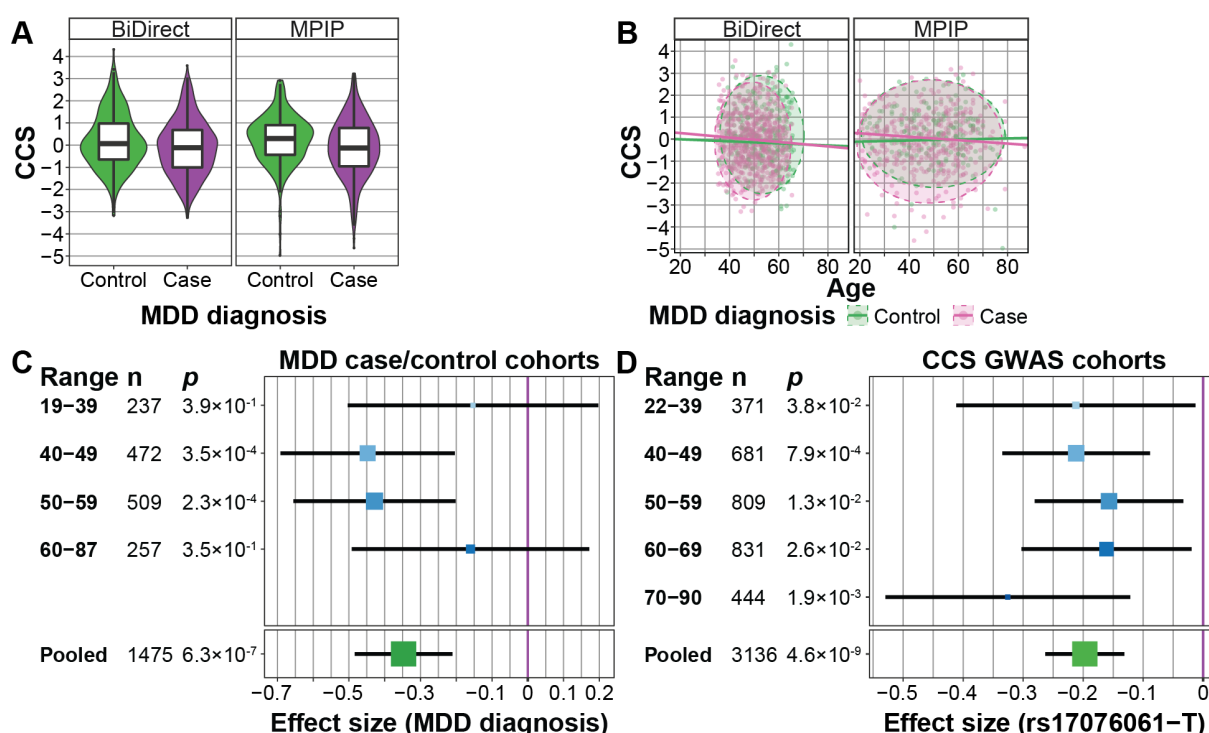
10

Figure 3: MDD-specific and age-dependent analyses of the CCS.
A: MDD cases had a significantly smaller CSS in two MDD cohorts (pooled $p=3\times10^{-6}$).
B: When a diagnosis-by-age interaction term was added to the regression model, the association of MDD diagnosis with CCS was not significant anymore; the interaction term was also not significant. **C:** Association of diagnosis with CCS across four age groups (combined sample of both MDD cohorts, the cohort was a covariate in the regression models). **D:** Association of SNP rs17076061 with CCS across five age groups (combined sample of all five GWAS cohorts, the cohort was a covariate).

Discussion

The CCS is a volumetric MRI-based marker associated with several psychiatric disorders (1). We conducted a GWAS and follow-up analyses to characterize genetic factors influencing the CCS and their relationship to psychiatric disorders. These analyses produced three main findings:

First, the minor allele T of the intergenic variant rs17076061 was associated with a decreased CCS at genome-wide significance and replicated. The SNP locates in between two predicted, uncharacterized long intergenic non-coding RNAs (lincRNA). The closest protein-coding genes to this SNP are "biorientation of chromosomes in cell division 1" (*BOD1*) and "stanniocalcin 2"

(*STC2*), 75 kbp downstream and 202 kbp upstream of SNP rs17076061, respectively.

BOD1 is a regulator of protein phosphatase 2A during cell division and, post-mitotically, a modulator of neuronal function (62): During the cell cycle, *BOD1*-mutant cells showed an accelerated progression through mitosis. BOD1 localized to presynapses in murine neurons and, in *Drosophila*, neuron-specific knockdown of *BOD1* using RNAi caused non-associative learning deficits and abnormal morphology of neuromuscular junctions. Furthermore, alterations at the *BOD1* locus might be associated with psychiatric disorders (62, 63): A mutation in *BOD1* co-segregated

11

with intellectual disability in a consanguineous family and somatic deletions in *BOD1* have been identified in neuronal samples from a schizophrenia patient, including tissue from the prefrontal cortex.

STC2 is a secreted glycoprotein with a possible auto- or paracrine function. In the regulation of apoptosis, the unfolded protein response promotes the expression of potentially neuroprotective STC2 in neuronal cells (64–66). Its homolog STC1, a regulator of neuronal, intracellular calcium homeostasis, has been suggested as a biomarker for neurodegenerative disorders (67). SNP rs17076061 is part of a significant expression quantitative trait locus with *STC2* in the pancreas (p=2.2×10^{-6}; GTEx v7 (68)). For the CS regions, the most relevant result from GTEx was for the anterior cingulate cortex (BA24, p=0.03). This finding was not significant after correction for multiple testing, yet the sample size for this tissue was about half the one for pancreas.

SNP rs17076061 likely affects the alternative binding of two transcription factors: the CCS-associated minor allele T supports the binding of E2F, the major allele supports binding of EBF. Moreover, rs17076061 is located within an element that is evolutionarily constrained in mammals (69). In summary, the associated locus 5q35.2 harbors two protein-coding genes expressed in the brain with either psychiatric or neuroprotective functions.

Second, the neurodevelopmental pathway "SEMA3A-Plexin repulsion signaling by inhibiting Integrin adhesion" was significantly associated with the CCS. Semaphorin-3A (SEMA3A) is a chemorepellent mediating axon guidance and a chemoattractant for dendrite growth, and plexins are the signal-transducing subunits of the SEMA3A receptor. The pathway is important during neuronal regeneration after brain trauma

(70) and SEMA3A and its receptor are associated with impaired tissue regeneration in chronic white matter multiple sclerosis lesions (71). Both Semaphorin-3A and Plexin A2 are relevant for different psychiatric disorders (72–75), supporting a broader, transdiagnostic function of the pathway: SEMA3A may contribute to neurodegeneration in Alzheimer's disease (73). It is upregulated in the brain of schizophrenia patients and has been suggested to contribute to the synaptic pathology of the disorder (72). *Plexin A2* (*PLXNA2*), one of the 13 gene-set members, is associated with schizophrenia, anxiety, and depression (74, 75) and is relevant for associate learning; *Plxna2*-deficient mice showed impaired neurogenesis and altered synaptic morphology (76). Of note, the *SEMA3A* homolog *SEMA5A* has been implicated in autism and intellectual diability (77, 78).

Third, we did not find evidence for a systematic overlap between the genetic architecture of the CCS and major psychiatric disorders. Neither was the top-associated variant rs17076061 directly associated with risk for psychiatric disorders in any of the examined GWAS nor were CCS PRS significantly higher in MDD cases. Moreover, PRS for psychiatric disorders were not significantly associated with the CCS after correction for multiple testing. However, the PRS for cross-disorder psychiatric risk was positively correlated with the CCS at nominal significance.

This lack of a genetic overlap with psychiatric disorders might seem contradictory at first sight, but this finding is in line with previous studies that found either no or only a weak, nominally significant genetic correlation between either subcortical volumes and schizophrenia or hippocampal volume and MDD, respectively (22, 23). A meta-analysis of genetic factors influencing

subcortical volumes with 40,000 individuals identified a significant genetic correlation between BD and the nucleus accumbens and the caudate nucleus, but no such correlation for schizophrenia (10). Interestingly, a recent study described an age-dependent association of schizophrenia PRS with cortical thickness of the salience network, a similar brain phenotype (79). Importantly, the analysis of a genetic overlap, as conducted by us and others (22, 23), investigated genome-wide similarities between GWAS. If only some variants showed a joint association or different loci exhibited mixed effect directions, the methods used here could be failing to detect similarities.

Several explanations are compatible with the finding that individuals at high polygenic risk for disease did not show a significantly reduced CCS. First, genetic factors shaping the CCS might contribute to disease risk without exhibiting strong univariate, additive effects, as tested for in our GWAS. This explanation is plausible because both the CCS variance explained by diagnostic status (R^2=1.9% in BiDirect and 3.7% in MPIP) and by rs17076061 (R^2=1.2%, sample size-weighted mean across cohorts) were small. Thus, any direct correlation between the SNP and MDD or other diagnoses would be expected to be low. Second, the CS regions might constitute a vulnerable brain network for psychiatric disorders. In this case, CCS-associated variants could increase the risk for GM loss in these regions, likely in interaction with other risk constellations, e.g., age or prolonged psychosocial stress. Thereby, smaller CS volumes might lead to brain dysfunction in susceptible individuals and specifically influence clinical presentations, e.g., cognitive functions. Interestingly, the CS regions represent nodes of the salience network, and CCS-associated SNPs might indirectly influence the structural integrity of this network, leading to deficits in achieving flexible cognitive control (80).

The model in which CS regions represent regional vulnerability is supported by our observation of a possible non-linear influence of age on the association of the CCS with MDD. Non-linear aging trajectories of volumetric measures are a known phenomenon, e.g., for subcortical brain structures (81, 82). Importantly, the studies analyzed in Goodkind *et al.* (1) assumed a common aging model between MDD cases and controls. Hence, latent group-by-age effects may have influenced their result, and their proposed neurobiological substrate could contain effects of accelerated aging in psychiatric patients (7). This might explain why the association of rs17076061 with the CCS varied by age, despite correction of the GM volumes for age effects.

The CS brain regions could thus be subject to accelerated brain aging in psychiatric patients, and rs17076061 could increase the risk for this phenomenon. Such an interaction between age and disorder is conceivable since we detected no genetic overlap between CCS-associated SNPs and genetic factors influencing EAA or longevity. Interestingly, the salience network is critically involved in accelerated cognitive decline during aging (83). Cognitive correlates of the CS have also been demonstrated in the original study by Goodkind *et al.* (1). Although the salience network is specifically prone to degeneration in bvFTD (84, 85), no overlap between CCS- and bvFTD-associated genetic variants was found. This observation once more suggests that a translation of the rs17076061 effects into an accelerated aging phenotype either occurs in interaction with other genetic risk factors or in the context of established psychiatric disease.

13

Our overall results pattern also indicate that transdiagnostic markers may adhere to the endophenotype concept even less clearly than imaging markers with higher clinical specificity. Whether rs17076061 is associated with brain volume differences during normal aging, in the context of psychiatric disorders, or with differential aging in psychiatric patients, should be followed up in a large-scale longitudinal brain imaging study, along with functional MRI analyses.

Acknowledgments

References

1. Goodkind M, Eickhoff SB, Oathes DJ, Jiang Y, Chang A, Jones-Hagata LB, *et al.* (2015): Identification of a Common Neurobiological Substrate for Mental Illness. *JAMA Psychiatry*. 72: 305–315.

2. Smeland OB, Wang Y, Frei O, Li W, Hibar DP, Franke B, *et al.* (2017): Genetic Overlap between Schizophrenia and Volumes of Hippocampus, Putamen, and Intracranial Volume Indicates Shared Molecular Genetic Mechanisms. *Schizophr Bull*. 44: 854–864.

3. van Erp T, Hibar D, Rasmussen J, Glahn D, Pearlson G, Andreassen O, *et al.* (2015): Subcortical brain volume abnormalities in 2028 individuals with schizophrenia and 2540 healthy controls via the ENIGMA consortium. *Mol Psychiatry*. 21: 547–553.

4. Hoogman M, Bralten J, Hibar DP, Mennes M, Zwiers MP, Schweren LS, *et al.* (2017): Subcortical brain volume differences in participants with attention deficit hyperactivity disorder in children and adults: a cross-sectional mega-analysis. *The Lancet Psychiatry*. 4: 310–319.

5. Schmaal L, Veltman D, van Erp T, Sämann P, Frodl T, Jahanshad N, *et al.* (2016): Subcortical brain alterations in major depressive disorder: findings from the ENIGMA Major Depressive Disorder working group. *Mol Psychiatry*. 21: 806.

6. Hibar D, Westlye L, van Erp T, Rasmussen J, Leonardo C, Faskowitz J, *et al.* (2016): Subcortical volumetric abnormalities in bipolar disorder. *Mol Psychiatry*. 21: 1710.

7. Koutsouleris N, Davatzikos C, Borgwardt S, Gaser C, Bottlender R, Frodl T, *et al.* (2014): Accelerated Brain Aging in Schizophrenia and Beyond: A Neuroanatomical Marker of Psychiatric Disorders. *Schizophr Bull*. 40: 1140–1153.

8. van Erp T, Walton E, Hibar DP, Schmaal L, Jiang W, Glahn DC, *et al.* (2018): Cortical Brain Abnormalities in 4474 Individuals With Schizophrenia and 5098 Control Subjects via the Enhancing Neuro Imaging Genetics Through Meta Analysis (ENIGMA) Consortium. *Biol Psychiatry*. 84: 644–654.

9. Schmaal L, Hibar D, Sämann P, Hall G, Baune B, Jahanshad N, *et al.* (2016): Cortical abnormalities in adults and adolescents with major depression based on brain scans from 20 cohorts worldwide in the ENIGMA Major Depressive Disorder Working Group. *Mol Psychiatry*. 22: 900.

10. Satizabal CL, Adams HH, Hibar DP, White CC, Stein JL, Scholz M, *et al.* (2017): Genetic Architecture of Subcortical Brain Structures in Over 40,000 Individuals Worldwide. *bioRxiv*. 173831.

11. Hibar DP, Adams HH, Jahanshad N, Chauhan G, Stein JL, Hofer E, *et al.* (2017): Novel genetic loci associated with hippocampal volume. *Nat Commun*. 8: 13624.

12. Hibar DP, Stein JL, Renteria ME, Arias-Vasquez A, Desrivières S, Jahanshad N, *et al.* (2015): Common genetic variants influence human subcortical brain structures. *Nature*. 520: 224.

13. Peper JS, Brouwer RM, Boomsma DI, Kahn RS, Pol HE (2007): Genetic influences on human brain structure: A review of brain imaging studies in twins. *Human Brain Mapping*. 28: 464–473.

14. Brouwer RM, Hedman AM, van Haren N, Schnack HG, Brans R, Smit D, *et al.* (2014): Heritability of brain volume change and its relation to intelligence. *NeuroImage*. 100: 676–683.

15. Elliott LT, Sharp K, Alfaro-Almagro F, Shi S, Miller KL, Douaud G, *et al.* (2018): Genome-wide association studies of brain imaging phenotypes in UK Biobank. *Nature*. 562: 210–216.

16. Zhao B, Ibrahim JG, Li Y, Li T, Wang Y, Shan Y, *et al.* (2018): Heritability of Regional Brain Volumes in Large-Scale Neuroimaging and Genetic Studies. *Cereb Cortex*. doi: 10.1093/cercor/bhy157 .

17. Uddin LQ (2014): Salience processing and insular cortical function and dysfunction. *Nat Rev Neurosci*. 16: nrn3857.

18. Pettersson E, Lichtenstein P, Larsson H, Song J, of the and of the of the of the of the of the of the Consortium S, Agrawal A, *et al.* (2019): Genetic influences on eight psychiatric disorders based on family data of 4 408 646 full and half-siblings, and genetic data of 333 748 cases and controls. *Psychol Med*. 49: 1166–1173.

19. The Brainstorm Consortium, Anttila V, Bulik-Sullivan B, Finucane HK, Walters RK, Bras J, *et al.* (2018): Analysis of shared heritability in common disorders of the brain. *Science* 360. doi: 10.1126/science.aap8757 .

20. Cross-Disorder Group of the Psychiatric Genomics Consortium, Lee PH, Anttila V, Won H, Feng Y-CA, Rosenthal J, *et al.* (2019): Genome wide meta-analysis identifies genomic relationships, novel loci, and pleiotropic mechanisms across eight psychiatric disorders. *BioRxiv*. 528117.

21. Cross-Disorder Group of the Psychiatric Genomics Consortium (2013): Genetic relationship between five psychiatric disorders estimated from genome-wide SNPs. *Nat Genet*. 45: 984–994.

22. Franke B, Stein JL, Ripke S, Anttila V, Hibar DP, van Hulzen KJ, *et al.* (2016): Genetic influences on schizophrenia and subcortical brain volumes: large-scale proof of concept. *Nat Neurosci*. 19: 420–431.

23. Wigmore E, Clarke T-K, Howard D, Adams M, Hall L, Zeng Y, *et al.* (2017): Do regional brain volumes and major depressive disorder share genetic architecture? A study of Generation Scotland (n=19 762), UK Biobank (n=24 048) and the English Longitudinal Study of Ageing (n=5766). *Transl Psychiatry*. 7: e1205.

24. Reus L, Shen X, Gibson J, Wigmore E, Ligthart L, Adams M, *et al.* (2017): Association of polygenic risk for major psychiatric illness with subcortical volumes and white matter integrity in UK Biobank. *Sci Rep.* 7: 42140.

25. Caspers S, Moebus S, Lux S, Pundt N, Schütz H, Mühleisen TW, *et al.* (2014): Studying variability in human brain aging in a population-based German cohort— rationale and design of 1000BRAINS. *Front Aging Neurosci.* 6: 149.

26. Roski C, Caspers S, Lux S, Hoffstaedter F, Bergs R, Amunts K, Eickhoff SB (2014): Activation shift in elderly subjects across functional systems: an fMRI study. *Brain Struct Funct.* 219: 707–718.

27. Teismann H, Wersching H, Nagel M, Arolt V, Heindel W, Baune BT, *et al.* (2014): Establishing the bidirectional relationship between depression and subclinical arteriosclerosis – rationale, design, and characteristics of the BiDirect Study. *BMC Psychiatry.* 14: 174.

28. Völzke H, Alte D, Schmidt C, Radke D, Lorbeer R, Friedrich N, *et al.* (2011): Cohort Profile: The Study of Health in Pomerania. *Int J Epidemiol.* 40: 294–307.

29. Hermesdorf M, Berger K, Szentkirályi A, Schwindt W, Dannlowski U, Wersching H (2017): Reduced fractional anisotropy in patients with major depressive disorder and associations with vascular stiffness. *Neuroimage Clin.* 14: 151–155.

30. Hennings JM, Owashi T, Binder EB, Horstmann S, Menke A, Kloiber S, *et al.* (2009): Clinical characteristics and treatment outcome in a representative sample of depressed inpatients – Findings from the Munich Antidepressant Response Signature (MARS) project. *J Psychiatr Res.* 43: 215–229.

31. Inkster B, Nichols TE, Saemann PG, Auer DP, Holsboer F, Muglia P, Matthews PM (2009): Association of GSK3β Polymorphisms With Brain Structural Changes in Major Depressive Disorder. *Arch Gen Psychiat.* 66: 721–728.

32. Ashburner J, Friston KJ (2005): Unified segmentation. *NeuroImage.* 26: 839–851.

33. Ashburner J (2007): A fast diffeomorphic image registration algorithm. *NeuroImage.* 38: 95–113.

34. Ising M, Lucae S, Binder EB, Bettecken T, Uhr M, Ripke S, *et al.* (2009): A Genomewide Association Study Points to Multiple Loci That Predict Antidepressant Drug Treatment Outcome in Depression. *Arch Gen Psychiat.* 66: 966–975.

35. Howard DM, Adams MJ, Clarke T-K, Hafferty JD, Gibson J, Shirali M, *et al.* (2019): Genome-wide meta-analysis of depression identifies 102 independent variants and highlights the importance of the prefrontal brain regions. *Nat Neurosci.* 1–10.

36. Caspers S, Röckner ME, Jockwitz C, Bittner N, Teumer A, Herms S, *et al.* (2019):

Pathway-specific genetic risk for Alzheimer's disease differentiates regional patterns of cortical atrophy in older adults. *Cereb Cortex*. in press.

37. Chang CC, Chow CC, Tellier L, Vattikuti S, Purcell SM, Lee JJ (2015): Second-generation PLINK: rising to the challenge of larger and richer datasets. *GigaScience*. 4: 7.

38. Gao F, Chang D, Biddanda A, Ma L, Guo Y, Zhou Z, Keinan A (2015): XWAS: A Software Toolset for Genetic Data Analysis and Association Studies of the X Chromosome. *J Hered*. 106: 666–671.

39. Howie B, Fuchsberger C, Stephens M, Marchini J, Abecasis GR (2012): Fast and accurate genotype imputation in genome-wide association studies through pre-phasing. *Nat Genet*. 44: 955.

40. Howie BN, Donnelly P, Marchini J (2009): A Flexible and Accurate Genotype Imputation Method for the Next Generation of Genome-Wide Association Studies. *PLOS Genet*. 5: e1000529.

41. Delaneau O, Zagury J-F, Marchini J (2013): Improved whole-chromosome phasing for disease and population genetic studies. *Nat Methods*. 10: 5.

42. Andlauer TF, Buck D, Antony G, Bayas A, Bechmann L, Berthele A, *et al.* (2016): Novel multiple sclerosis susceptibility loci implicated in epigenetic regulation. *Sci Adv*. 2: e1501678.

43. Yang J, Benyamin B, McEvoy BP, Gordon S, Henders AK, Nyholt DR, *et al.* (2010): Common SNPs explain a large proportion of the heritability for human height. *Nat Genet*. 42: 565.

44. Yang J, Lee HS, Goddard ME, Visscher PM (2011): GCTA: A Tool for Genome-wide Complex Trait Analysis. *Am J Hum Gen*. 88: 76–82.

45. Willer CJ, Li Y, Abecasis GR (2010): METAL: fast and efficient meta-analysis of genomewide association scans. *Bioinformatics*. 26: 2190–2191.

46. Machiela MJ, Chanock SJ (2015): LDlink: a web-based application for exploring population-specific haplotype structure and linking correlated alleles of possible functional variants. *Bioinformatics*. 31: 3555–3557.

47. Liberzon A, Birger C, Thorvaldsdóttir H, Ghandi M, Mesirov JP, Tamayo P (2015): The Molecular Signatures Database Hallmark Gene Set Collection. *Cell Syst*. 1: 417–425.

48. de Leeuw CA, Mooij JM, Heskes T, Posthuma D (2015): MAGMA: Generalized Gene-Set Analysis of GWAS Data. *PLOS Comput Biol*. 11: e1004219.

49. Segrè AV, Consortium D, investigators M, Groop L, Mootha VK, Daly MJ, Altshuler D (2010): Common Inherited Variation in Mitochondrial Genes Is Not

Enriched for Associations with Type 2 Diabetes or Related Glycemic Traits. *PLOS Genet*. 6: e1001058.

50. Cross-Disorder Group of the Psychiatric Genomics Consortium (2013): Identification of risk loci with shared effects on five major psychiatric disorders: a genome-wide analysis. *Lancet*. 381: 1371–1379.

51. Stahl EA, Breen G, Forstner AJ, McQuillin A, Ripke S, Trubetskoy V, *et al.* (2019): Genome-wide association study identifies 30 loci associated with bipolar disorder. *Nat Genet*. 51: 793–803.

52. Wray NR, Ripke S, Mattheisen M, Trzaskowski M, Byrne EM, Abdellaoui A, *et al.* (2018): Genome-wide association analyses identify 44 risk variants and refine the genetic architecture of major depression. *Nat Genet*. 50: 668–681.

53. Schizophrenia Working Group of the Psychiatric Genomics Consortium, Ripke S, Neale BM, Corvin A, Walters JT, Farh K-H, *et al.* (2014): Biological insights from 108 schizophrenia-associated genetic loci. *Nature*. 511: 421.

54. Ferrari R, Hernandez DG, Nalls MA, Rohrer JD, Ramasamy A, Kwok JB, *et al.* (2014): Frontotemporal dementia and its subtypes: a genome-wide association study. *Lancet Neurol*. 13: 686–99.

55. Deelen J, Beekman M, Uh H-W, Broer L, Ayers KL, Tan Q, *et al.* (2014): Genome-wide association meta-analysis of human longevity identifies a novel locus conferring survival beyond 90 years of age. *Hum Mol Genet*. 23: 4420–4432.

56. Lu AT, Hannon E, Levine ME, Crimmins EM, Lunnon K, Mill J, *et al.* (2017): Genetic architecture of epigenetic and neuronal ageing rates in human brain regions. *Nat Commun*. 8: 15353.

57. Andlauer TF, Guzman-Parra J, Streit F, Strohmaier J, Gonzalez M, Flores S, *et al.* (2018): Bipolar multiplex families have an increased burden of common risk variants for psychiatric disorders. *BioRxiv*. 468975.

58. Bulik-Sullivan BK, Loh P-R, Finucane HK, Ripke S, Yang J, of the Consortium S, *et al.* (2015): LD Score regression distinguishes confounding from polygenicity in genome-wide association studies. *Nat Genet*. 47: ng.3211.

59. Bulik-Sullivan B, Finucane HK, Anttila V, Gusev A, Day FR, Loh P-R, *et al.* (2015): An atlas of genetic correlations across human diseases and traits. *Nat Genet*. 47: 1236–1241.

60. Plaisier SB, Taschereau R, Wong JA, Graeber TG (2010): Rank–rank hypergeometric overlap: identification of statistically significant overlap between gene-expression signatures. *Nucleic Acids Res*. 38: e169–e169.

61. The 1000 Genomes Project Consortium, Gibbs RA, Boerwinkle E, Doddapaneni H, Han Y, Korchina V, *et al.* (2015): A global reference for human genetic variation.

Nature. 526: 68.

62. Esmaeeli-Nieh S, Fenckova M, Porter IM, Motazacker MM, Nijhof B, Castells-Nobau A, *et al.* (2016): BOD1 Is Required for Cognitive Function in Humans and Drosophila. *PLOS Genet*. 12: e1006022.

63. Kim J, Shin J-Y, Kim J-I, Seo J-S, Webster MJ, Lee D, Kim S (2014): Somatic deletions implicated in functional diversity of brain cells of individuals with schizophrenia and unaffected controls. *Sci Rep*. 4: 3807.

64. Volland S, Kugler W, Schweigerer L, Wilting J, Becker J (2009): Stanniocalcin 2 promotes invasion and is associated with metastatic stages in neuroblastoma. *Int J C International Journal of Cancer ancer*. 125: 2049–2057.

65. Ito D, Walker JR, Thompson CS, Moroz I, Lin W, Veselits ML, *et al.* (2004): Characterization of Stanniocalcin 2, a Novel Target of the Mammalian Unfolded Protein Response with Cytoprotective Properties. *Mol Cell Biol*. 24: 9456–9469.

66. Byun J-S, Lee J-W, Kim S, Kwon K, Sohn J-H, Lee K, *et al.* (2010): Neuroprotective effects of stanniocalcin 2 following kainic acid-induced hippocampal degeneration in ICR mice. *Peptides*. 31: 2094–2099.

67. Shahim P, Blennow K, Johansson P, Svensson J, Lista S, Hampel H, *et al.* (2017): Cerebrospinal Fluid Stanniocalcin-1 as a Biomarker for Alzheimer's Disease and Other Neurodegenerative Disorders. *Neuromolecular Med*. 19: 154–160.

68. Melé M, Ferreira PG, Reverter F, DeLuca DS, Monlong J, Sammeth M, *et al.* (2015): The human transcriptome across tissues and individuals. *Science*. 348: 660–665.

69. Ward LD, Kellis M (2016): HaploReg v4: systematic mining of putative causal variants, cell types, regulators and target genes for human complex traits and disease. *Nucleic Acids Res*. 44: D877–D881.

70. Mecollari V, Nieuwenhuis B, Verhaagen J (2014): A perspective on the role of class III semaphorin signaling in central nervous system trauma. *Front Cell Neurosci*. 8: 328.

71. Costa C, Martínez-Sáez E, Gutiérrez-Franco A, Eixarch H, Castro Z, Ortega-Aznar A, *et al.* (2015): Expression of semaphorin 3A, semaphorin 7A and their receptors in multiple sclerosis lesions. *Mult Scler*. 21: 1632–1643.

72. Eastwood S, Law A, Everall I, Harrison P (2003): The axonal chemorepellant semaphorin 3A is increased in the cerebellum in schizophrenia and may contribute to its synaptic pathology. *Mol Psychiatry*. 8: 4001233.

73. Good PF, Alapat D, Hsu A, Chu C, Perl D, Wen X, *et al.* (2004): A role for semaphorin 3A signaling in the degeneration of hippocampal neurons during Alzheimer's disease. *Journal Neurochem*. 91: 716–736.

74. Wray NR, James MR, Mah SP, Nelson M, Andrews G, Sullivan PF, *et al.* (2007): Anxiety and Comorbid Measures Associated With PLXNA2. *Arch Gen Psychiatry*. 64: 318–326.

75. Mah S, Nelson M, DeLisi L, Reneland R, Markward N, James M, *et al.* (2006): Identification of the semaphorin receptor PLXNA2 as a candidate for susceptibility to schizophrenia. *Mol Psychiatry*. 11: 471.

76. Zhao X-F, Kohen R, Parent R, Duan Y, Fisher GL, Korn MJ, *et al.* (2018): PlexinA2 Forward Signaling through Rap1 GTPases Regulates Dentate Gyrus Development and Schizophrenia-like Behaviors. *Cell Rep.* 22: 456–470.

77. Mosca-Boidron A-L, Gueneau L, Huguet G, Goldenberg A, Henry C, Gigot N, *et al.* (2015): A de novo microdeletion of SEMA5A in a boy with autism spectrum disorder and intellectual disability. *Eur J Hum Genet*. 24: 838–843.

78. Weiss LA, Arking DE, Daly MJ, Chakravarti A, Arking DE, Brune CW, *et al.* (2009): A genome-wide linkage and association scan reveals novel loci for autism. *Nature*. 461: 802.

79. Alloza C, Blesa-Cábez M, Bastin ME, Madole JW, Buchanan CR, Janssen J, *et al.* (2019): Psychotic-like experiences, polygenic risk scores for schizophrenia and structural properties of the salience, default mode and central-executive networks in healthy participants from UK Biobank. *BioRxiv*. 729921.

80. Menon V (2015): Salience Network. In: Toga AW, ed. *Brain Mapping: An Encyclopedic Reference*. Academic Press. 2015;2:597-611.

81. Ziegler G, Dahnke R, Jäncke L, Yotter R, May A, Gaser C (2012): Brain structural trajectories over the adult lifespan. *Hum Brain Mapp*. 33: 2377–2389.

82. Fjell AM, Westlye LT, Grydeland H, Amlien I, Espeseth T, Reinvang I, *et al.* (2013): Critical ages in the life course of the adult brain: nonlinear subcortical aging. *Neurobiol Aging*. 34: 2239–2247.

83. Corte V, Sperduti M, Malherbe C, Vialatte F, Lion S, Gallarda T, *et al.* (2016): Cognitive Decline and Reorganization of Functional Connectivity in Healthy Aging: The Pivotal Role of the Salience Network in the Prediction of Age and Cognitive Performances. *Front Aging Neurosci*. 8: 204.

84. Seeley WW, Crawford RK, Zhou J, Miller BL, Greicius MD (2009): Neurodegenerative Diseases Target Large-Scale Human Brain Networks. *Neuron*. 62: 42–52.

85. Pievani M, Pini L, Ferrari C, Pizzini FB, Galazzo I, Cobelli C, *et al.* (2010): Coordinate-Based Meta-Analysis of the Default Mode and Salience Network for Target Identification in Non-Invasive Brain Stimulation of Alzheimer's Disease and

Behavior Variant Frontotemporal Dementia Networks. *J Alzheimers Dis*. 57: 825–843.

Behavior Variant Frontotemporal Dementia Networks. *J Alzheimers Dis*. 57: 825–843.

A

B

Region ● Left AIC ● Right AIC ● dACC

C

Left AIC

Right AIC

dACC

CCS

D

GWAS workflow

VBM pre-processing of T1-weighted images
with NLO Jacobian modulation

↓

Extraction of regional volumes (AIC and dACC)

↓

ROI-wise **correction** for covariates
in a linear model

↓

Calculation of **PCA** based on residuals

↓

GWAS (**linear regression**) with
ancestry components as covariates

↓

Discovery-stage fixed-effects **meta-analysis**

↓

Replication of variants with $p<5\times10^{-8}$
in LD blocks via fixed-effects meta-analysis

A 5q35.2

B Correlation (r^2)

		$p_{Disc.}$	$p_{Repl. (1s)}$
rs10068178		4.2×10^{-8}	
rs10076027		4.0×10^{-8}	
rs10053202		4.0×10^{-8}	
rs2339961		3.5×10^{-8}	
rs2161352		3.5×10^{-8}	
rs2112619		2.2×10^{-8}	
rs17076061		$\mathbf{1.5\times10^{-8}}$	$\mathbf{9.9\times10^{-3}}$
rs7700692		1.4×10^{-8}	
rs17052028		1.8×10^{-8}	
rs36014631		1.3×10^{-8}	
rs72088023		$\mathbf{1.1\times10^{-8}}$	7.5×10^{-2}
rs880915		4.8×10^{-8}	

Position on chr. 5 (Mbp)   172.96   172.98   173.0

C rs17076061

D

	p		
1000BRAINS	3.6×10^{-4}		Discovery
CONNECT100	9.0×10^{-1}		
BiDirect	1.9×10^{-2}		
SHIP-0	8.8×10^{-2}		
Discovery	1.5×10^{-8}		D.P.
SHIP-Trend	2.8×10^{-2}		Repl.
Pooled	3.4×10^{-6}		Pool

Effect size (rs17076061–T)

A

B

C

MDD case/control cohorts

Range	n	p
19–39	237	$3.9×10^{-1}$
40–49	472	$3.5×10^{-4}$
50–59	509	$2.3×10^{-1}$
60–87	257	$3.5×10^{-1}$
Pooled	1475	$6.3×10^{-7}$

Effect size (MDD diagnosis)

D

CCS GWAS cohorts

Range	n	p
22–39	371	$3.8×10^{-2}$
40–49	681	$7.9×10^{-4}$
50–59	809	$1.3×10^{-1}$
60–69	831	$2.6×10^{-2}$
70–90	444	$1.9×10^{-3}$
Pooled	3136	$4.6×10^{-9}$

Effect size (rs17076061−T)